



Effects of Viscous Dissipation and Chemical Reaction on Nonlinear convective Flow of a Casson Fluid between Vertical Channel

¹P. Naveen, ²Ch. Ramreddy

^{1,2}Department of Mathematics,

National Institute of Technology Warangal-506004, India

¹naveenpadi09@gmail.com, ²chittetiram@gmail.com

Abstract: The aim of the present communication is to investigate the chemical reaction and viscous dissipation effects on the nonlinear convective flow of a Casson fluid through the vertical channel. In addition, the nonlinear temperature-concentration-dependent density relation (i.e. nonlinear convection or nonlinear Boussinesq approximation) takes into account. Adomian decomposition method (ADM) was applied to find the solutions to the problem and the numerical results validated by the novel successive linearization method. The emerging physical parameters on the flow characteristics are discussed through tabular form and graphical representations.

Keywords: Casson fluid, Nonlinear Boussinesq approximation, Adomian decomposition method.

I. INTRODUCTION

Various scientific models have been proposed in the past couple of decades to acquire an intensive perception of the mechanics of non-Newtonian fluids. Since non-Newtonian fluids have significant applications in food preservation techniques, power engineering, petroleum production, and chemical process industries. Casson fluid is one and it can be selected to fit the rheological behavior of tomato sauce, soup, honey, and jelly. Casson fluid model can also be the most compatible formulation to simulate blood type fluid flow and it exhibits yield stress in the constitutive equation (Casson, 1959). Very important contributions to the flow problems characterizing Casson fluid can be found in the works of Attia and Sayed-Ahmed (2010), Shehzad et al. (2013). The combined effect of viscous dissipation and first-order chemical reaction on the convective heat and mass transport in non-Newtonian fluid flow over different geometries has been a great concept interest for many investigators (Shateyi et al., 2010; Barik and Dash, 2014; Ahmed et al., 2017). Very recently Gireesha et al. (2019) studied the effect of cross-diffusion and viscous dissipation on the mixed convective flow of Casson fluid over a vertical plate.

In some investigations related to the heat and mass transfer, it is essential to consider nonlinear density temperature (NDT) and nonlinear density concentration

(NDC) variations in the buoyancy term. Heat released by the viscous dissipation triggers some changes in density gradients.

Vajravelu and Sastri (1977) reported that the NDT variation in flow between two parallel walls affects the flow and heat transfer rates to a large extent. Casson fluid flow past a heated horizontal wall in the presence of NDT variation and viscous dissipation has been studied by Shaw et al. (2016). Recent advances in this direction in non-Newtonian fluid flow can be seen in the studies of Hayat et al. (2018) and Srinivasacharya et al. (2018). The present study aims to provide a discussion of the combined viscous dissipation and chemical reaction on the nonlinear convective flow of a Casson fluid along a vertical channel. In spite of the complex structure of the problem and to provide more accurate results, the final nonlinear system of equations is solved using the Adomian Decomposition Method (ADM). ADM is a generally new methodology, which gives an analytic approximation to linear and nonlinear problems. It requires neither linearization nor perturbation and furthermore, it gives the solution as an infinite series in which each term can be determined. Interesting features of the present setup has been given at the end of the study.

II. MATHEMATICAL ANALYSIS

Consider the fully developed Casson fluid flow through a vertical channel. Under the standard boundary layer assumptions and with nonlinear Boussinesq approximation (Hayat et al., 2014; Shaw et al., 2016; Ajayi et al., 2017 and RamReddy et al. 2018), the governing equations are

$$\frac{\partial \tilde{v}}{\partial \tilde{y}} = 0 \quad (1)$$

The associated conditions are given by

$$\text{At } \tilde{y} = -\tilde{d} : \tilde{u} = 0, \tilde{T} = \tilde{T}_1, \tilde{C} = \tilde{C}_1; \text{ and at } \tilde{y} = \tilde{d} : \tilde{u} = 0, \tilde{T} = \tilde{T}_2, \tilde{C} = \tilde{C}_2 \quad (5)$$

In the above equations, the dimensional parameters are given by density as ρ , specific heat as \tilde{C}_p , coefficients of thermal expansion of first and second orders as δ_1 and δ_2 , coefficients of solutal expansion of first and second orders as δ_3 and δ_4 , respectively, thermal diffusivity as α , mass diffusivity as D ,

Introducing the new variables in the dimensionless form

$$Y = \frac{\tilde{y}}{d}, F = \frac{\tilde{u}}{\tilde{u}_0}, R = \frac{\tilde{v}_0 d}{\nu}, T = \frac{\tilde{T} - \tilde{T}_0}{\tilde{T}_2 - \tilde{T}_0}, A = -\frac{d^2}{\mu \tilde{u}_0} \frac{dp}{d\tilde{x}}, C = \frac{\tilde{C} - \tilde{C}_0}{\tilde{C}_2 - \tilde{C}_0} \quad (6)$$

Substitute Eq. (6) in Eqs. (1)-(5), the dimensionless governing equations are

$$\left(1 + \frac{1}{\beta}\right) \frac{d^2 F}{dY^2} - R \frac{dF}{dY} - A + \frac{Gr}{Re} [(1 + \Omega_1 T)T + N_c (1 + \Omega_2 C)C] = 0 \quad (7)$$

$$\frac{d^2 F}{dY^2} - R \Pr \frac{dT}{dY} + Br \left(1 + \frac{1}{\beta}\right) \left(\frac{dF}{dY}\right)^2 = 0 \quad (8)$$

$$\frac{d^2 C}{dY^2} - R Sc \frac{dC}{dY} - \lambda Sc C = 0 \quad (9)$$

The transformed boundary conditions in dimensionless form

$$F = 0, T = R_t, C = R_s \text{ at } Y = -1 \text{ and } F = 0, T = 1, C = 1 \text{ at } Y = 1 \quad (10)$$

The dimensionless parameters like Reynolds number (Re), suction/injection parameter (R), Prandtl number (\Pr), Schmidt number (Sc), Grashof number (Gr), non-dimensional chemical reaction parameter (λ), Brinkman number (Br), constant pressure gradient (A), Buoyancy ratio (N_c), nonlinear-density-temperature parameter (NDT) (Ω_1), Eckert number (Ec),

$$\tilde{v} \frac{\partial \tilde{u}}{\partial \tilde{y}} = \nu \left(1 + \frac{1}{\beta}\right) \frac{\partial^2 \tilde{u}}{\partial \tilde{y}^2} + g \left[\delta_1 (\tilde{T} - \tilde{T}_0) + \delta_2 (\tilde{T} - \tilde{T}_0)^2 + \delta_3 (\tilde{C} - \tilde{C}_0) + \delta_4 (\tilde{C} - \tilde{C}_0)^2 \right] + \frac{1}{\rho} \frac{\partial p}{\partial \tilde{x}} \quad (2)$$

$$\tilde{v} \frac{\partial \tilde{T}}{\partial \tilde{y}} = \alpha \frac{\partial^2 \tilde{T}}{\partial \tilde{y}^2} + \frac{\nu}{\tilde{C}_p} \left(1 + \frac{1}{\beta}\right) \left(\frac{\partial \tilde{u}}{\partial \tilde{y}}\right)^2 \quad (3)$$

$$\tilde{v} \frac{\partial \tilde{C}}{\partial \tilde{y}} = D \left[\frac{\partial^2 \tilde{C}}{\partial \tilde{y}^2}\right] - K_1 (\tilde{C} - \tilde{C}_0) \quad (4)$$

acceleration due to gravity as g , first-order chemical reaction parameter as K_1 , pressure gradient as \tilde{p} , Casson fluid parameter as β , coefficient of viscosity as μ , velocity components along the \tilde{x} and \tilde{y} directions as \tilde{u} and \tilde{v} , respectively,

$$\begin{aligned} \text{Re} &= \frac{u_0 d}{\nu}, \text{Pr} = \frac{\nu}{\alpha}, \text{Sc} = \frac{\nu}{D}, \text{Gr} = \frac{g \delta_1 d^3}{\nu^2} (\tilde{T}_2 - \tilde{T}_0), \lambda = \frac{K_1 d^2}{\nu}, \text{Br} = \text{Pr} \text{Ec} = \frac{\mu \tilde{u}_0^2}{(\tilde{T}_2 - \tilde{T}_0)}, \\ N_c &= \frac{\delta_3 (\tilde{C}_2 - \tilde{C}_0)}{\delta_1 (\tilde{T}_2 - \tilde{T}_0)}, \Omega_1 = \frac{\delta_2 (\tilde{T}_2 - \tilde{T}_0)}{\delta_1}, \text{Ec} = \frac{\tilde{u}_0^2}{C_p (\tilde{T}_2 - \tilde{T}_0)} \text{ and } \Omega_2 = \frac{\delta_4 (\tilde{C}_2 - \tilde{C}_0)}{\delta_3} \end{aligned} \quad (11)$$

The physical quantities of present interest (i.e. heat and mass transfer rates on the left side and right side walls) in dimensionless form are represented as

$$Nu_1 = \frac{dT}{dY} \Big|_{Y=-1}, \quad Sh_1 = \frac{dC}{dY} \Big|_{Y=-1}, \quad Nu_2 = \frac{dT}{dY} \Big|_{Y=1} \quad \text{and} \quad Sh_2 = \frac{dC}{dY} \Big|_{Y=1} \quad (12)$$

III. ANALYTICAL PROCEDURE VIA ADM

3.1 Fundamentals of ADM

In view of the basic methodology involved, we consider a general non-linear differential equation:

$$G[u(t)] = r(t) \quad (13)$$

where $u(t)$ is the unknown function, $r(t)$ is the source term and G represents a general nonlinear ordinary or partial differential operator including both linear and nonlinear terms.

Let us rewrite the equation (13) into the standard operator form as follows:

$$Lu + \mathfrak{N}u + \mathfrak{R}u = r \quad (14)$$

where L is usually the highest order derivative (which easily invertible), \mathfrak{R} is the remainder of the linear operator and $\mathfrak{N}u$ indicates the nonlinear terms.

Applying the inverse operator L^{-1} (which is a twofold indefinite integral) on both sides of (14) and by using the associated boundary conditions. One can obtain the unknown function $u(t)$ as

$$u(t) = Q - L^{-1}[\mathfrak{R}u] - L^{-1}[\mathfrak{N}u] \quad (15)$$

Here Q represents the sum of the twofold integral result of $r(t)$ and terms from the auxiliary conditions.

The standard ADM defines the solution u and nonlinear $\square u$ term by the infinite series as

$$\begin{aligned} LF &= R \left(\frac{\beta}{1 + \beta} \right) \frac{dF}{dY} + A \left(\frac{\beta}{1 + \beta} \right) - \frac{Gr}{\text{Re}} \left(\frac{\beta}{1 + \beta} \right) [(1 + \Omega_1 T)T + N_c (1 + \Omega_2 S)S] \\ LT &= R \text{Pr} \frac{dT}{dY} - Br \left(1 + \frac{1}{\beta} \right) \left(\frac{dF}{dY} \right)^2 \\ LS &= R \text{Sc} \frac{dS}{dY} + \lambda \text{Sc} S \end{aligned} \quad (20)$$

$$u = \sum_{k=0}^{\infty} u_k \quad \text{and} \quad \mathfrak{N}u = \sum_{k=0}^{\infty} A_k \quad (16)$$

where A_k are the special Adomian polynomials which are obtained recursively from the following relation.

$$A_k = \frac{1}{k!} \left[\frac{d^k}{d\lambda^k} \left[\mathfrak{N} \left(\sum_{i=0}^k \lambda^i u_i \right) \right] \right]_{\lambda=0}, \quad k = 0, 1, 2, \dots \quad (17)$$

Therefore, the solution of Eq. (13) is given by

$$\sum_{k=0}^{\infty} u_k = Q - L^{-1} \left(\mathfrak{R} \sum_{k=0}^{\infty} u_k \right) - L^{-1} \left(\sum_{k=0}^{\infty} A_k \right) \quad (18)$$

By expanding the series (18) and comparing the coefficients of u_0, u_1, u_2, \dots . We get the following recurrence relations

$$\left. \begin{aligned} u_0 &= Q \\ \vdots \\ u_{k+1} &= -L^{-1} \mathfrak{R} u_k - L^{-1} A_k \end{aligned} \right\} \quad (19)$$

Using (17), (18) and (19), we can compute all the

$$u = \sum_{k=0}^{\infty} u_k \quad \text{components } u_k \text{ and hence} \quad .$$

3.2 A solution of the Fluid Equations

The present section is devoted to solving fluid equations (7) to (9) by following the above said steps of Adomian decomposition Method (Aski et al., 2014). According to Eq. (14), Eqs. (7) to (9) can be written as

Where, L is the second order operator and its inverse operator is defined as

$$L^{-1} = \int_{-1}^Y \int_{-1}^Y (\cdot) dY dY$$

$$\begin{aligned}
 F(Y) &= F(0) + F'(0)Y + L^{-1} \left\{ \left(\frac{\beta}{1+\beta} \right) \left[R \frac{dF}{dY} + A - \frac{Gr}{Re} [(1+\Omega_1 T)T + N_c (1+\Omega_2 S)S] \right] \right\} \\
 T(Y) &= T(0) + T'(0)Y + L^{-1} \left[R \Pr \frac{dT}{dY} - Br \left(1 + \frac{1}{\beta} \right) \left(\frac{dF}{dY} \right)^2 \right] \\
 S(Y) &= S(0) + S'(0)Y + L^{-1} \left[R Sc \frac{dS}{dY} + \lambda Sc S \right]
 \end{aligned} \tag{21}$$

Next, we decompose the required solution as an infinite sum given below

$$\begin{aligned}
 F(Y) &= \sum_{m=0}^{\infty} F_m(Y) = F_0(Y) + L^{-1}(\aleph_1) \\
 T(Y) &= \sum_{m=0}^{\infty} T_m(Y) = T_0(Y) + L^{-1}(\aleph_2) \\
 S(Y) &= \sum_{m=0}^{\infty} S_m(Y) = S_0(Y) + L^{-1}(\aleph_3)
 \end{aligned} \tag{22}$$

and the nonlinear terms are decomposed into a series of Adomian polynomials as

$$\begin{aligned}
 \aleph_1(F) &= \left(\frac{\beta}{1+\beta} \right) \left\{ R \frac{dF}{dY} + A - \frac{Gr}{Re} [(1+\Omega_1 T)T + N_c (1+\Omega_2 S)S] \right\} = \sum_{n=0}^{\infty} B_n(F) \\
 \aleph_2(T) &= R \Pr \frac{dT}{dY} - Br \left(1 + \frac{1}{\beta} \right) \left(\frac{dF}{dY} \right)^2 = \sum_{n=0}^{\infty} C_n(T) \\
 \aleph_3(S) &= R Sc \frac{dS}{dY} + \lambda Sc S = \sum_{n=0}^{\infty} D_n(S)
 \end{aligned} \tag{23}$$

where $\sum_{n=0}^{\infty} B_n(F)$, $\sum_{n=0}^{\infty} C_n(T)$, and $\sum_{n=0}^{\infty} D_n(S)$ are Adomian polynomials.

To determine the components of $F_m(Y)$, $T_m(Y)$ and $S_m(Y)$, the initial values of $F_0(Y)$, $T_0(Y)$ and $S_0(Y)$ are obtained with the boundary conditions.

$$\begin{aligned}
 F_0(Y) &= F(0) + F'(0)Y = a_1 + a_2 Y, \quad T_0(Y) = T(0) + T'(0)Y = a_3 + a_4 Y, \\
 S_0(Y) &= S(0) + S'(0)Y = a_5 + a_6 Y
 \end{aligned} \tag{24}$$

Using Eq. (22) and Eq. (23) into Eq. (21), we obtain

$$F_1(Y) = \left(1 + \frac{1}{\beta} \right) \left\{ \begin{aligned}
 &\left[R a_2 + A - \frac{Gr}{Re} [a_3 + \Omega_1 a_3^2 + N_c a_5 + N_c \lambda_2 a_5^2] \right] \frac{Y^2}{2} - \frac{Gr}{Re} (a_4 + 2\Omega_1 a_3 a_4) \frac{Y^3}{6} - \\
 &\left[\frac{Gr}{Re} (N_c a_6 + 2N_c \Omega_2 a_5 a_6) \frac{Y^3}{6} - \left[\frac{Gr}{Re} (\Omega_1 a_4^2 + N_c \Omega_2 a_6^2) \right] \frac{Y^4}{12} \right]
 \end{aligned} \right\} \tag{25}$$

By applying the inverse differential operator on both sides of the set of Eqs. (20) leads to

$$T_1(Y) = \left[R \Pr a_4 - Br \left(1 + \frac{1}{\beta} \right) (a_2^2) \right] \frac{Y^2}{2} \quad (26)$$

$$S_1(Y) = [R Sc a_6 + \lambda Sc a_5] \frac{Y^2}{2} + \lambda Sc a_6 \frac{Y^3}{6} \quad (27)$$

Further, $F_m(Y)$, $T_m(Y)$ and $S_m(Y)$ for $m \geq 2$ be determined in similar way from. Finally, the approximate solution can be achieved with following series expansions.

$$F(Y) = \sum_{m=0}^{\infty} F_m(Y), T(Y) = \sum_{m=0}^{\infty} T_m(Y), S(Y) = \sum_{m=0}^{\infty} S_m(Y) \quad (28)$$

IV. RESULTS AND DISCUSSIONS

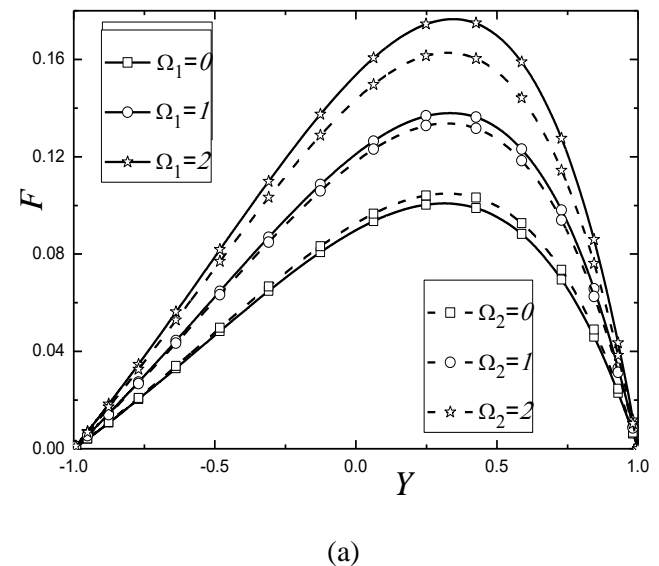
The results obtained by Adomian Decomposition Method were well matched with the results carried out by a novel successive linearization method (Motsa et al., 2011), as shown in Table 1. This numerical comparison reveals that the error in results is at an acceptable level. The effects of Casson fluid parameter (β), NDT parameter (Ω_1), NDC parameter (Ω_2),

chemical reaction parameter (λ) and Brinkman Number (Br), and slip constants (Rt and Rc) on the fluid profiles are exhibited through Figs 1 to 4. For this the numerical computations are carried out by taking $R = 2.0$, $Gr = 10$, $Re = 2.0$, $N_c = 0.5$, $A = 1.0$, $Pr = 0.72$, $Sc = 0.22$, $Rt = 0.1$ and $Rs = 0.1$.

Table 1: Comparison of Nu_1 , Nu_2 , Sh_1 and Sh_2 between ADM and SLM									
Pr	ADM		SLM		Sc	ADM		SLM	
	Nu_1	Nu_2	Nu_1	Nu_2		Sh_1	Sh_2	Sh_1	Sh_2
0.72	1.9722	0.2992	1.9723	0.2991	0.22	1.3055	0.6032	1.3056	0.6033
2.97	7.9549	0.0042	7.9550	0.0042	0.6	2.1346	0.2716	2.1347	0.2717
4.24	11.3969	0.0017	11.3970	0.0017	0.96	3.0263	0.1080	3.0266	0.1080
7	18.8582	0.0009	18.8583	0.0009	2	5.8414	-0.0205	5.8415	-0.0205

Figure 1(a) depicts the influence of Ω_1 and Ω_2 parameters on the Casson fluid velocity and it reveals that fluid velocity increases with by enhancing these two parameters from zero to some positive value. Also, observed that the fluid velocity more in the presence of these parameters as compared to its absence results.

Physically, $\Omega_1 > 0$ and $\Omega_2 > 0$ implies that $\tilde{T}_1 > \tilde{T}_0$ and $\tilde{C}_1 > \tilde{C}_0$; hence, there will be a supply of heat and mass to the flow region from the wall. Due to this exchange, there is an increase in velocity with the presence of Ω_1 and Ω_2 . Influence of Casson parameter (β) on the velocity of the fluid is projected in Fig. 1(b) for both linear and nonlinear convection cases. It is worth to mention that an increase in β reduces the yield stress which offers very less resistance to the fluid motion. This effectively facilitates the flow of the fluid in the middle of the channel, as shown in Fig. 1(b).



(a)

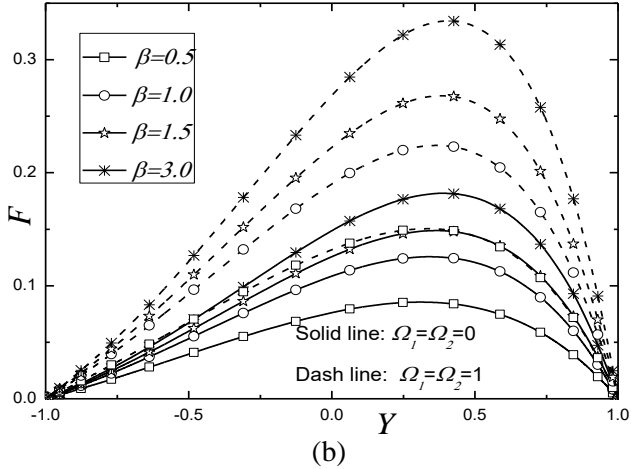


Figure 1: Variation of velocity (a) with Ω_1 and Ω_2 , (b) with β .

Effect of chemical reaction parameter λ on the velocity and concentration is projected in the Figs. 2(a) and 2(b), respectively. Since a rise in λ will control species concentration and it leads to reduce the chemical molecular diffusivity, i.e., less diffusion. This destructive reaction reduces the velocity and concentration of the Casson fluid with the increase of λ , shown in above said projections.

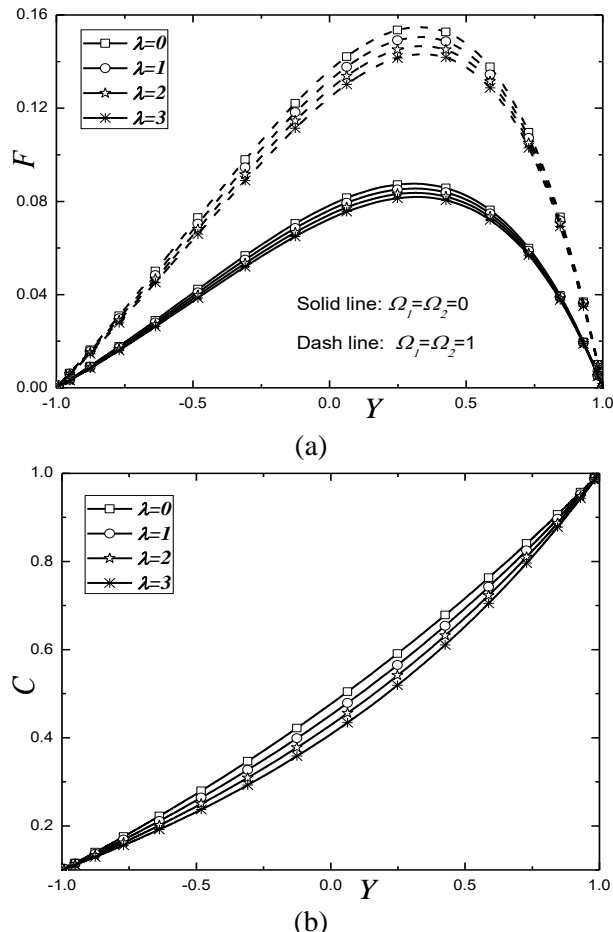


Figure 2: Variation of (a) velocity, and (b) concentration with λ .

Variation of velocity and temperature with Brinkman number (Br) is identified in the Figs. 3(a) and 3(b), respectively. The rise in Br , slow down the conduction of heat which is generated by viscous dissipation and this reduction favor the velocity and temperature of the fluid, as shown in Figs. 3(a) and 3(b). In the last set of Figs. 4(a) and 4(b), the influence of slip parameters is considered on the respective distributions (i.e., temperature with Rt and in other concentration with Rs). Increase in the respective slip parameters there is a huge in both temperature and concentration as depicted in Figs. 4(a) and 4(b).

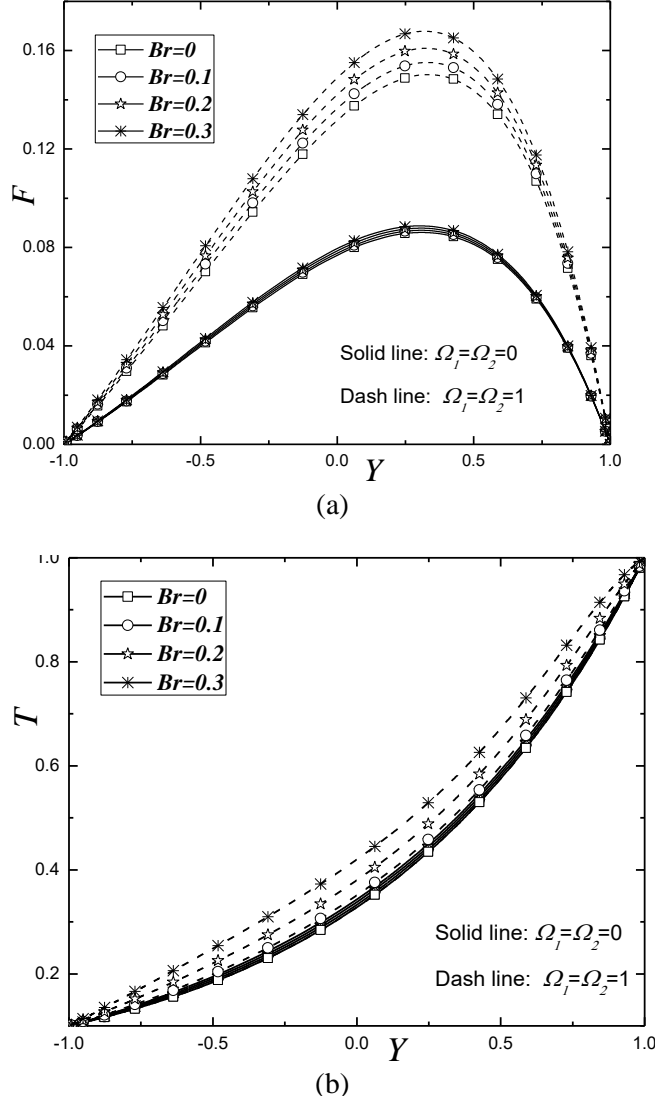
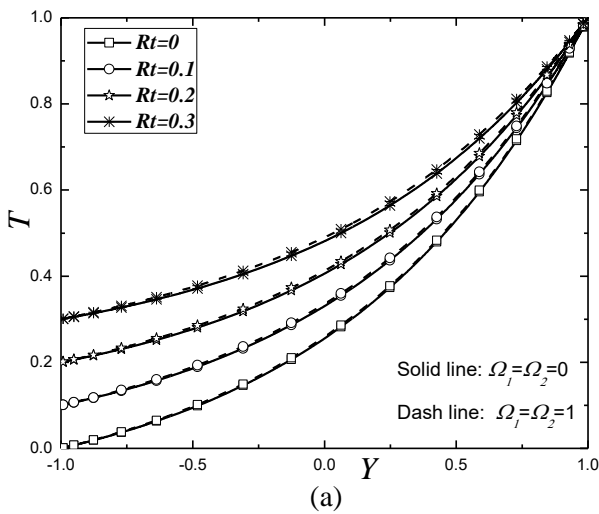


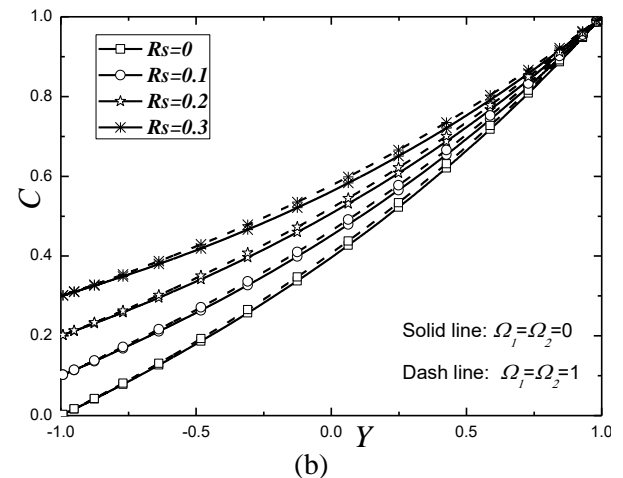
Figure 3: Variation of (a) velocity, and (b) temperature with Br .

The variation of Nusselt number and Sherwood number (where Nusselt number represents the heat transfer rate and Sherwood number represents the mass transfer rates) with effects of Casson fluid parameter (β), chemical reaction parameter (λ) and the Brinkman Number (Br) at both the left and right side walls are exhibited in Table 2. A rise in β leads to decrease the Nusselt number at the left side wall while it intensifies

at the right side wall. There is no effect of β on the Sherwood number on both the left side as well as right side walls with β . Taking the constant values of $\beta = 1.0$, $Br = 2.0$, both the Nusselt number and Sherwood numbers are a decline on the right side wall while they increase on the left side wall, with an increase in λ . Also with an increase of Br , the heat transfer rate magnify on the left side wall while it shows the reverse trend on the right side wall, but Sherwood number do not have influence with Br on both the walls.



(a)



(b)

Figure 4: (a) Variation of temperature with R_t and (b) Variation of concentration with R_s .

Finally, the above all figures are depicted to identify the impact of pertinent parameters on the flow of Casson fluid along a vertical channel in both linear and nonlinear convections. Also, Nusselt number and Sherwood numbers are measured in the absence and presence of nonlinear convection parameters, as given in Table 2. From the above investigations, it is noticed that the influence of the pertinent parameters is enhanced by the presence of nonlinear convection parameters. Due to the presence of nonlinear gradients in the buoyancy term, the impact of pertinent parameters is improved and it shows a larger influence on the behavior fluid characteristics compared with linear convection results.

Table 2: Effect of β , λ , Br on the Nusselt and Sherwood numbers at both left and right sides of walls for both linear and nonlinear convection cases.

		Linear convection ($\Omega_1 = \Omega_2 = 0$)				Nonlinear convection ($\Omega_1 = \Omega_2 = 1$)			
		Nu_1	Nu_2	Sh_1	Sh_2	Nu_1	Nu_2	Sh_1	Sh_2
β	0.1	2.1948	0.2541	1.3055	0.6032	2.1889	0.2555	1.3055	0.6032
	0.2	2.1884	0.2556	1.3055	0.6032	2.1683	0.2600	1.3055	0.6032
	0.3	2.1799	0.2575	1.3055	0.6032	2.1409	0.2655	1.3055	0.6032
λ	1	2.1604	0.2612	1.3055	0.6032	2.0769	0.2770	1.3055	0.6032
	2	2.1611	0.2610	1.3795	0.5725	2.0797	0.2762	1.3795	0.5725
	3	2.1618	0.2608	1.4513	0.5430	2.0823	0.2755	1.4513	0.5430
Br	1	2.1604	0.2612	1.3055	0.6032	2.0769	0.2770	1.3055	0.6032
	2	2.1227	0.2693	1.3055	0.6032	1.9491	0.3023	1.3055	0.6032
	3	2.0843	0.2775	1.3055	0.6032	1.8130	0.3298	1.3055	0.6032

V. CONCLUSION

Major findings of the present study are summarized below:

- Velocity and Nusselt numbers enhanced at the right side wall while the Nusselt number at the left side wall decreases, as Casson fluid parameter increases.

- Heat and mass transfer rates at the left and right side of the walls increase with an increase of both nonlinear convection parameters.
- Both the F and T of the Casson fluid increased with the Br and Rt .
- Velocity and concentration profiles are increasing functions of λ and Rs .

Conflict of Interest

Both the authors have equal contribution in this work and it is declared that there is no conflict of interest for this publication.

Acknowledgment

The authors express their sincere gratitude to the referees for their valuable suggestions towards the improvement of the paper.

References

[1] Ahmed, S., Zueco, J., & Lopez-Gonzalez, L. M. (2017). Effects of chemical reaction, heat and mass transfer and viscous dissipation over a MHD flow in a vertical porous wall using perturbation method. *International Journal of Heat and Mass Transfer*, 104, 409-418.

[2] Ajayi, T. M., Omowaye, A. J., & Animasaun, I. L. (2017). Viscous dissipation effects on the motion of Casson fluid over an upper horizontal thermally stratified melting surface of a paraboloid of revolution: boundary layer analysis. *Journal of Applied Mathematics*, 2017. Article ID 1697135, 13 pages.

[3] Aski, F. S., Nasirkhani, S. J., Mohammadian, E., & Asgari, A. (2014). Application of Adomian decomposition method for micropolar flow in a porous channel. *Propulsion and Power Research*, 3(1), 15-21.

[4] Attia, H. A., & Sayed-Ahmed, M. E. (2010). Transient MHD Couette flow of a Casson fluid between parallel plates with heat transfer. *Italian Journal of Pure and Applied Mathematics*, 27, 19-38.

[5] Barik, R. N., & Dash, G. C. (2014). Thermal radiation effect on an unsteady magnetohydrodynamic flow past inclined porous heated plate in the presence of chemical reaction and viscous dissipation. *Applied Mathematics and Computation*, 226, 423-434.

[6] Casson, N. (1959). A flow equation for pigment-oil suspensions of the printing ink type. *Rheology of Disperse Systems*, 84-104.

[7] Gireesha, B. J., Kumar, K. G., Krishnamurthy, M. R., Manjunatha, S., & Rudraswamy, N. G. (2019). Impact of ohmic heating on MHD mixed convection flow of Casson fluid by considering Cross diffusion effect. *Nonlinear Engineering*, 8(1), 380-388.

[8] Hayat, T., Asad, S., & Alsaedi, A. (2014). Flow of variable thermal conductivity fluid due to inclined stretching cylinder with viscous dissipation and thermal radiation. *Applied Mathematics and Mechanics*, 35(6), 717-728.

[9] Hayat, T., Khan, M. W. A., Khan, M. I., Waqas, M., & Alsaedi, A. (2018). Impact of chemical reaction in fully developed radiated mixed convective flow between two rotating disk. *Physica B: Condensed Matter*, 538, 138-149.

[10] Motsa, S. S., Sibanda, P., & Shateyi, S. (2011). On a new quasi-linearization method for systems of nonlinear boundary value problems. *Mathematical Methods in the Applied Sciences*, 34(11), 1406-1413.

[11] RamReddy, C., Naveen, P., & Srinivasacharya, D. (2018). Nonlinear convective flow of non-Newtonian fluid over an inclined plate with convective surface condition: a Darcy-Forchheimer model. *International Journal of Applied and Computational Mathematics*, 4(1), 51-68.

[12] Shateyi, S., Motsa, S. S., & Sibanda, P. (2010). Homotopy analysis of heat and mass transfer boundary layer flow through a non-porous channel with chemical reaction and heat generation. *The Canadian Journal of Chemical Engineering*, 88(6), 975-982.

[13] Shaw, S., Mahanta, G., & Sibanda, P. (2016). Non-linear thermal convection in a Casson fluid flow over a horizontal plate with convective boundary condition. *Alexandria Engineering Journal*, 55(2), 1295-1304.

[14] Shehzad, S. A., Hayat, T., Qasim, M., & Asghar, S. (2013). Effects of mass transfer on MHD flow of Casson fluid with chemical reaction and suction. *Brazilian Journal of Chemical Engineering*, 30(1), 187-195.

[15] Srinivasacharya, D., RamReddy, C., & Naveen, P. (2018). Double dispersion effect on nonlinear convective flow over an inclined plate in a micropolar fluid saturated non-Darcy porous medium. *Engineering Science and Technology, an International Journal*, 21(5), 984-995.

[16] Vajravelu, K., & Sastri, K. S. (1977). Fully developed laminar free convection flow between two parallel vertical walls—I. *International Journal of Heat and Mass Transfer*, 20(6), 655-660.